PHYSICAL REVIEW B, VOLUME 65, 081402(R)

Reconstruction and energetics of the polar (112) and $(\overline{1}\overline{1}2)$ versus the nonpolar (220) surfaces of $CuInSe_2$

S. B. Zhang and S.-H. Wei
National Renewable Energy Laboratory, Golden, Colorado 80401
(Received 17 October 2001; published 8 February 2002)

First-principles total-energy calculation reveals a number of (112) and $(\overline{1}\overline{1}2)$ surface structures stable at different atomic chemical potentials. All of the stable structures are charge compensated, thus semiconducting, either by cation-on-cation antisites, cation vacancies, Se adatoms, or by Se addimers. This structural richness raises the possibility for engineering $CuInSe_2/Cu(In_{1-x}Ga_x)Se_2$ material properties by surface control during the growth. The experimentally observed puzzling spontaneous decomposition of the (220)/(204) surfaces into (112) and $(\overline{1}\overline{1}2)$ is also confirmed by calculating individual surface energies.

DOI: 10.1103/PhysRevB.65.081402 PACS number(s): 68.35.Md, 68.35.Bs

$CuInSe_2$ (CIS) and related alloys are important ternary optoelectronic materials.[1] Polycrystalline CIS is exclusively used in the solar cell technology. Due to the large density of the grains, the efficiency of the multigrain heterojunction solar cells depends sensitively on the physical properties of the CIS surfaces. For example, recent studies of the $CuIn_{1-x}Ga_xSe_2$ (CIGS) solar cells reveal[2] that certain surface orientation [e.g., (220)] of the CIGS thin films might have superior properties over others. CIS surfaces also show some unusual physical properties, not seen on binary surfaces. A recent atomic force microscopy (AFM) study[3] showed that the CIGS (220)/(204) surfaces are unstable against spontaneous decomposition into the (112) and $(\overline{1}\overline{1}2)$ facets. The physical origin of such a puzzling surface instability remains a mystery. Cation sublattice stacking faults were observed[4] in molecular-beam epitaxy grown CIS. It was suggested that the stacking faults nucleate at the growing surface under the Cu-rich conditions. To understand how the surface might affect the electronic, as well as the structural properties of the CIS/CIGS films, it is essential to determine the stable surface structures.

Using the first-principles total-energy approach, we have calculated the various atomic structures of the $(112)/(\overline{1}\overline{1}2)$ surfaces. A number of them were found stable at different atomic chemical potentials. All of the stable structures are semiconducting, as they are fully charge-compensated either by cation-on-cation antisites, cation vacancies, Se adatoms, or by Se addimers. This suggests that self-compensation is a general concept that applies to a wide range of semiconductor surfaces from III-V,[5] to II-VI,[6,7] and now to I-III-VI_2. The surface structural richness raises the possibility for engineering $CuInSe_2/Cu(In_{1-x}Ga_x)Se_2$ material properties by control of the surface reconstruction during the growth. The physical origin of the puzzling spontaneous decomposition of the (220)/(204) surfaces into (112) and $(\overline{1}\overline{1}2)$ is explained by the formation of CIS specific defects, in particular, the subsurface In-on-Cu antisites on the anion-terminated $(\overline{1}\overline{1}2)$ surface.

The calculation was carried out using the pseudopotential approach under the local-density approximation,[8] as implemented in the VASP code[9] with the Vanderbilt ultrasoft pseudopotentials.[10] We used supercells to mimic the $(112)/(\overline{1}\overline{1}2)$ surfaces, which contain 12 atomic layers +4 vacuum layers. A 180 eV cutoff energy was used and tested up to 234 eV. At least four special **k** points in the x-y plane are used in the calculations. Atoms at the back surface are fixed while the rest of them are relaxed until the forces are less than 0.1 eV/Å. Absolute surface energies are calculated. Details will be given elsewhere.[11] The calculation for the (220) and (204) surfaces is done with supercells of 16 and 8 atomic layers, respectively, +4 vacuum layers. The uncertainties are estimated to be $\pm 0.1\ \mathrm{eV}/a_0^2$ for the absolute energy, and $\pm 0.02\ \mathrm{eV}/a_0^2$ for energy difference between different reconstructions, where a_0 is the calculated bulk lattice constant$=5.72$ Å.

It is well known that semiconductor surface energy is a sensitive function of the sample preparation/growth conditions. These translate[5] into the dependence on the atomic chemical potentials. For ternary CIS, there are two independent chemical potentials:[12] μ_{Cu} and μ_{In}, whereas the chemical potential of Se can be determined by the heat of formation [$\Delta H_{CIS}=2.11$ eV (Ref. 13)] via $\mu_{Cu}+\mu_{In}+2\mu_{Se}=-\Delta H_{CIS}$. Figure 1 shows the triangle indicating the accessible region of the Cu and In chemical potentials. Given the

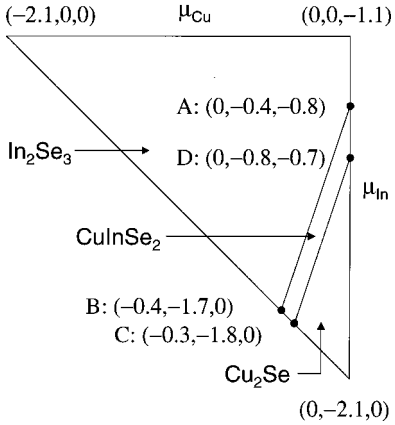

FIG. 1. Physically accessible region of the atomic chemical potentials, $(\mu_{Cu},\mu_{In},\mu_{Se})$. The CIS region is a narrow strip defined by the four corners *A-B-C-D*, at which the values of $(\mu_{Cu},\mu_{In},\mu_{Se})$ are given.

TABLE I. Calculated absolute surface-energies (in eV/a_0^2) at the four corner points (A–D) of CIS in Fig. 1. Surface coverage of Cu, In, and Se (η_{Cu}, η_{In}, η_{Se}) relative to ideal, bulk-truncated surface for the (112) and $(\overline{1}\overline{1}2)$ surfaces, are also calculated. For example, for the (112)-Cu_{In} surface one Cu is added to and one In is removed from a $c(4\times2)$ cell of four surface atoms, so $\eta_{Cu}=1/4$ and $\eta_{In}=-1/4$. For the Se addimer surfaces, two Se are added so that $\eta_{Se}=2/4=1/2$.

	A	B	C	D	η_{Cu}	η_{In}	η_{Se}
			(112) Surface				
Se_{AD}	1.21	1.21	1.21	1.21	0	0	1/4
$V_{Cu}+V_{In}$	0.93	0.93	0.93	0.93	−1/8	−1/8	0
Cu_{In}	1.00	1.00	0.90	0.90	1/4	−1/4	0
$2V_{Cu}$	0.89	0.89	0.98	0.98	−1/2	0	0
$2Cu_{AD}$	3.59	4.56	4.47	3.68	1/2	0	0
$In_{Cu}+2In_{AD}$	1.66	3.11	3.21	2.03	−1/4	3/4	0
Se addimer	1.46	0.98	0.98	1.37	0	0	1/2
			$(\overline{1}\overline{1}2)$ Surface				
Se_{AD}	2.12	1.16	1.16	1.94	0	0	1/4
In_{Cu}	0.91	0.91	1.00	1.00	−1/4	1/4	0
$2Cu_{AD}$	3.16	2.19	2.10	2.88	1/2	0	0
Se addimer	2.16	0.71	0.71	1.89	0	0	1/2
V_{Se}	1.72	1.72	1.72	1.72	0	0	−1/4

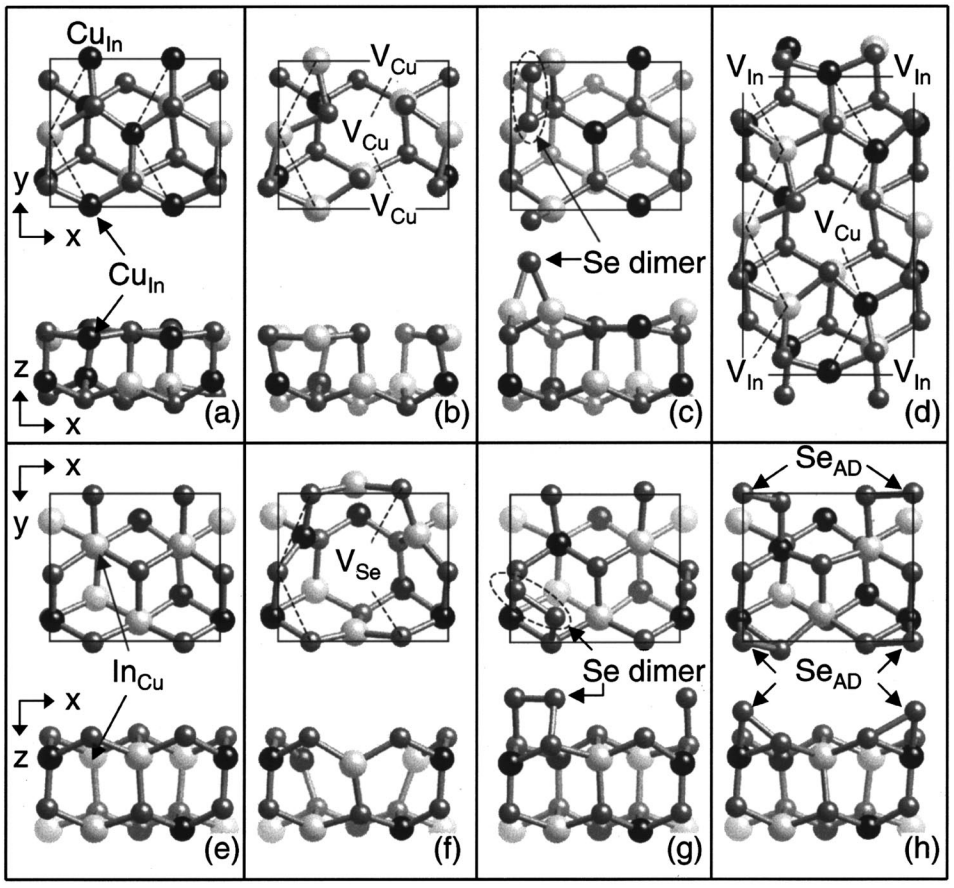

FIG. 2. Calculated atomic structures of the (112) [(a)–(d)], and $(\overline{1}\overline{1}2)$ [(e)–(h)] surfaces. Each panel contains two parts, the top view (top) and the side view (bottom), except for the (Cu, In) vacancy pair in (d) where only the top view is shown. The axes are $\mathbf{x}=[1\overline{1}0]$, $\mathbf{y}=[22\overline{2}]$, and $\mathbf{z}=[112]$. Dashed lines are used to connect the nominal top-surface atoms, and to indicate the location of the Se addimers. The black ball is Cu, the white ball is In, the smallest dark-gray ball is Se.

constraints that binary compounds In_2Se_3 and Cu_2Se also may form from the Cu-In-Se mixture, the triangle in Fig. 1 is further divided into three subregions. CIS is only a narrow stripe with four corners defined by *A-B-C-D*, indicating that μ_{Cu} and μ_{In} are quasidependent. In principle, the CIS region in Fig. 1 is further narrowed[12] by the formation of ordered vacancy compounds, 1-3-5, 1-5-7, etc. but these will not be considered here.

We name the surfaces using the convention for binary compounds. Thus, for the nonpolar (220) and (204) surfaces, the primitive unit cells are $c(2\times2)$ and 1×4, respectively. Similar to the binary (110) counterpart, these nonpolar surfaces have equal (Cu+In) and Se coverage, as well as equal Cu and In coverage. The calculated surface energies are 1.08 eV/a_0^2 for (220), and 1.16 eV/a_0^2 for (204), respectively. The slightly higher energy for the (204) surface reflects the fact that in the (220) surface, Cu and In form alternating chains along the [110] and [001] directions. In contrast, in the (204) surface, cations form Cu-Cu-In-In chains along the [102] direction, and Cu and In chains along the [010] direction, respectively. Upon charge transfer to Se,[14] Coulomb interaction among the charged surface cations is more repulsive for the (204) surface.

For the polar (112) and $(\bar{1}\bar{1}2)$ surfaces, the primitive unit cell is $c(4\times2)$. We considered twelve different structures for the cation-terminated (112): nine $c(4\times2)$ and three 4×2, and five structures for the anion-terminated $(\bar{1}\,\bar{1}\,2)$ all in $c(4\times2)$. Table I lists the absolute surface energies at points *A*, *B*, *C*, and *D* in Fig. 1, along with the surface coverage of the various chemical species. Figure 2 shows four lowest-energy structures for (112), (a) Cu-on-In (Cu_{In}) antisite, (b) 2 Cu vacancies ($2V_{Cu}$ equals complete depletion of Cu from surface layer), (c) Se addimer, and (d) (Cu, In) vacancy pair. The higher-energy structures not included in Fig. 2 are Se adatom (Se_{AD}), Cu adatom (Cu_{AD}), and $In_{AD}+2In_{Cu}$, where the adatom (AD) is on the H_3 site.[15] In contrast to Si(111),[15] we find that the $H3$ site is more stable than the $T4$ site typically by about 0.1 eV/a_0^2. In addition, we found that $2Cu_{AD}$ on surface Cu is unstable. This is consistent with the fact that Cu_{AD}-on-In in Table I has the highest energy. Figure 2 also shows four lowest-energy structures for $(\bar{1}\bar{1}2)$, (e) In-on-Cu (In_{Cu}) subsurface antisite, (f) Se vacancy (V_{Se}), (g) Se addimer, and (h) Se adatom (Se_{AD}). The only structure not included in Fig. 2 is Cu_{AD}. Not surprisingly, it also has a relatively high energy.

We found that surface Se atoms are threefold coordinated, which prefer the close-to 90° p^3 bond angle. Surface cation Cu and In atoms are also threefold coordinated, which, however, prefer the planar 120° sp^2 bond angle. These general trends are very similar to III-V (Ref. 5) and II-VI (Refs. 6,7) semiconductors. As a result of the cation relaxations, the top-surface cation layer is often below the topmost anion layer [see Fig. 2(a) and (b)]. In addition, we see the following in Fig. 2: (a) Cu_{In}. Due to the smaller size of Cu relative to In, the three nearest-neighbor Se atoms are displaced towards Cu_{In} by almost 0.3 Å. The tetrahedral Se bond angles are significantly reduced by up to 36°. (b) $2V_{Cu}$. Two of the four topmost Se atoms are twofold coordinated with an 89°-bond angle whereas the other two are threefold. (c) Se addimer. Here, the Se adatoms are twofold coordinated on top of In atoms. The Se-Se bondlength is 2.34 Å. The bond angles are, on the average, 103°. (d) V_{Se}. Surface relaxation leads to significant atomic displacements. (g) Se addimer on $(\bar{1}\,\bar{1}\,2)$. The Se-Se addimer bondlength is 2.26 Å whereas the Se-to-surface Se bondlength is 2.46 Å. The bondangles are about 102°. (h) Se_{AD}. This is the only metallic yet reasonably low-energy surface. The Se adatom is bonded to two Se, as well as one Cu in the subsurface layer. The fivefold-coordinated Cu causes the metallic behavior.

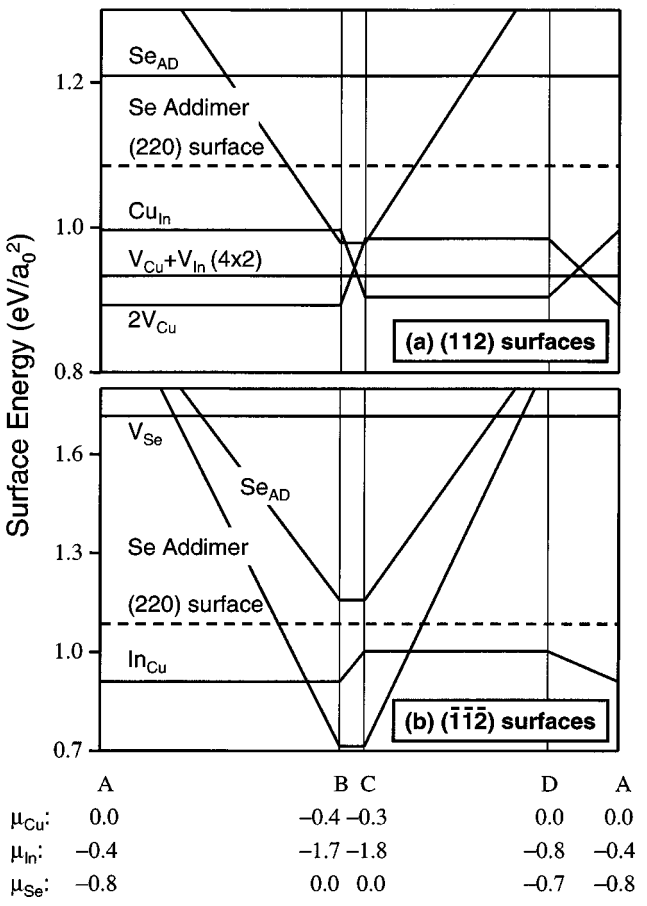

FIG. 3. The absolute surface energy for (a) (112) and (b) $(\bar{1}\,\bar{1}\,2)$ surfaces. The energy for the (220) surface is also shown in the dashed line for comparison. At the bottom, *A-B-C-D* refers to the four corners in Fig. 1 with their respective values given.

Figure 3 shows the calculated surface energies as a function of the atomic chemical potentials μ for low-energy structures. We see that surface reconstruction is sensitive to μ in the following. (*i*) The (112) surface.

(1) From *A* to *B*, the Cu-poor $2V_{Cu}$ is stable. From *C* to *D*, the In-poor Cu_{In} is stable. In Fig. 1, the *A-B* line is more In-rich (i.e., less negative μ_{In}) than the *C-D* line, explaining the change in the energy order between the two.

(2) The cation-poor (Cu, In)-vacancy pair also has low energy to within 0.04 eV/a_0^2 of either $2V_{Cu}$ or Cu_{In}, and is stable in regions where transition between the two is under the way.

(3) The energy of Se addimer goes down quite drastically

near points *B* and *C* (Se-rich). However, it is never low enough to become stable. (*ii*) The (1 1 2) surface.

(1) The Se addimer, being 0.7 eV/a_0^2 at the Se-rich limit, is by far the most stable surface structure.

(2) The In-rich In_{Cu} structure dominates over a large μ space and has the antisite in the *subsurface*, instead of the surface layer. Again, the *A-B* line is more In-rich than the *C-D* line. Thus, In_{Cu} has lower energy in *A-B* than *C-D*. Both (1) and (2) here are absent in the (112) surface. From the above results, we see the following.

(1) Even though in the literature[3] one often does not make the distinction between the (220) and (204) surfaces, we found that their energy difference can be significant due to an intrinsic difference in the surface Coulomb attraction.

(2) The polar (112) and (1 1 2) surfaces possess complex surface-structure ''phase diagrams.'' Such complexity raises the possibility for tailoring the physical properties of CIS films by imposing desired structures during the growth. For example for the (112) surface, growth along the *A-B* line would result in a Cu-vacancy rich environment. Even if a fraction of the surface vacancies can be buried to become bulk vacancies, it would naturally lead to *p*-type films. The same is true for the *C-D* line, which, however, provides a much deeper Cu_{In} double acceptor. This could be undesirable if achieving good *p*-typeness is the purpose, but could be desirable if semi-insulating is the purpose. For the (1 1 2) surface, the formation of the Se addimers will lead to a Se double layer that could interrupt the growth sequence, thereby causing surface roughness.[3] Finally, we note that self-compensation at the (112) surface is always achieved by intrinsic defects [16] that are *p* type in the bulk (V_{Cu}, Cu_{In}, and V_{In}), whereas for the (1 1 2) surface, it is always achieved by intrinsic defects that are *n* type in the bulk (In_{Cu}, Se antisites), instead.

(*iii*) Recently, Liao and Rockett[3] reported AFM observation of the spontaneous decomposition of the (220)/(204) surfaces into (112) and (1 1 2) facets. According to Fig. 3, the (220) [and the less stable (204)] surface is not only unstable against the average of (112) and (1 1 2) surfaces, but is also less stable against either one of them. Interestingly for the (112) surface, not only the structures involving CIS-specific defects such as V_{Cu} and Cu_{In} have lower energies, but also the (Cu, In)-vacancy pair. In comparison with CIS binary counterpart, ZnSe, the latter result suggests that even the cation-terminated (111) surface of ZnSe may have lower energy than the (110) surface by cation vacancy formation. On the other hand, the low energy of the (1 1 2) surface at least in the Se-poor condition is due entirely to the CIS-specific In_{Cu} antisites. Thus, spontaneous decomposition may not occur in ZnSe. Moreover, In_{Cu} is in the subsurface layer. Being fourfold-, instead of being threefold- coordinated, the diffusion barrier for In_{Cu} is expected to be much larger than threefold- or twofold-coordinated surface defects/adatoms. Hence, one has the opportunity to kinetically suppress In_{Cu} formation during the growth. This will force the (1 1 2) surface to be either Se vacancy or Se addimer terminated, preventing the decomposition of the (220) surface in the Se-poor condition: indeed at point *A* in Fig. 3, $[E(2V_{Cu})_{(112)}+E(V_{Se})_{\overline{(112)}}]/2$ is 0.22 eV/a_0^2 higher, instead of lower, than $E(220)$.

In summary, we have determined the stable atomic structures of the (112)/(1 1 2) surfaces as a function of the atomic chemical potentials. We found that self-compensation is a general principle that applies to a broad range of semiconductor surfaces from III-V, to II-VI, and to I-III-VI. The potential effects of surface self-compensation on the bulk properties of the CIS/CIGS films are discussed. Finally, we explain the spontaneous decomposition of the (220)/(204) surfaces into (112) and (1 1 2) facets. We thank R. Noufi, D. Liao for stimulating discussions, and A. Rockett for providing Ref. 3 prior to publication. This work was supported by the U.S. Department of Energy under Contract No. DE-AC98-GO10337 and by DOE/NERSC-supplied MPP computer time.

[1] J. L. Shey and J. H. Wernick, *Ternary Chalcopyrite Semiconductors* (Pergamon, Oxford, 1975).
[2] M. A. Contreras *et al.*, Prog. Photovoltaics Res. Appl. **7**, 311 (1999).
[3] D. Liao and A. Rockett, J. Appl. Phys. **91** (to be published).
[4] O. Hellman, S.-i. Tanaka, S. Niki, and P. Fons, J. Mater. Res. **11**, 1398 (1996).
[5] J. E. Northrup and S. Froyen, Phys. Rev. B **50**, 2015 (1994).
[6] C. H. Park and D. J. Chadi, Phys. Rev. B **49**, 16 467 (1994).
[7] A. Garcia and J. E. Northrup, Appl. Phys. Lett. **65**, 708 (1994).
[8] W. Kohn and L. J. Sham, Phys. Rev. **140**, A1133 (1965).
[9] G. Kresse and J. Hafner, Phys. Rev. B **47**, R558 (1993).
[10] D. Vanderbilt, Phys. Rev. B **41**, 7892 (1990).
[11] S. B. Zhang and S.-H. Wei (unpublished).
[12] S. B. Zhang, S.-H. Wei, and A. Zunger, Phys. Rev. Lett. **78**, 4059 (1997).
[13] D. Cahen and R. Noufi, J. Phys. Chem. Solids **53**, 991 (1992).
[14] S. B. Zhang and M. L. Cohen, Surf. Sci. **172**, 754 (1986).
[15] J. E. Northrup, Phys. Rev. Lett. **53**, 683 (1984).
[16] S. B. Zhang, S.-H. Wei, A. Zunger, and H. Katayama-Yoshida, Phys. Rev. B **57**, 9642 (1998).